Design of Dual-Band Miniaturized Frequency Selective Surface Using Branched Tortuous Structure

Ning Liu [1], Xianjun Sheng [2], Xiang Gao [2], Chunbo Zhang [3], and Dongming Guo [1]

[1] Department of Mechanical Engineering
Dalian University of Technology, Dalian, 116024, China
liuning@mail.dlut.edu.cn, guodm@dlut.edu.cn

[2] Department of Electrical Engineering
Dalian University of Technology, Dalian, 116024, China
568481055@qq.com, sxianjun@dlut.edu.cn

[3] Research Institute of Aerospace Special Materials and Processing Technology
Beijing, 100074, China
1628593171@qq.com

Abstract ─ A miniaturized dual-band frequency selective surface (FSS) is designed by using branched tortuous pattern of cross-dipole element backed by a wire grid of the same periodicity. By introducing the backing wire grid, the metallic line based FSS can provide two pass bands operating at 3.75GHz and 5.88GHz, respectively. The unit size of the proposed FSS is smaller than other similar FSSs and is only $0.075\lambda \times 0.075\lambda$ in size, where λ is the free-space wavelength at the first resonant frequency. Also, it shows good polarization stability and angular stability. Both simulated and measured results validate the performance.

Index Terms ─ Branched tortuous structure, dual band, frequency selective surface, periodic structure, miniaturization.

I. INTRODUCTION

Frequency selective surfaces (FSSs) are one- or two-dimensional periodic structures, which have been widely applied in the field of microwave to construct hybrid radome, antenna reflector, optical filter, electromagnetic shelter and so on [1-4]. Under some special applications, for example, multiband FSSs with independent transmission bands are required to increase the capacity of multi-frequency antenna in satellite communication system [5]. In practical applications mentioned above, FSSs are applied in limited space. To maintain the frequency selective property when applied in limited space, miniaturized FSSs are desired [6-8]. Hence, miniaturized multiband FSSs are highly demanded in practical applications.

Motivated by this requirement, different structures have been proposed to realize miniaturized dual-band or multiband FSS. Dual-band miniaturized FSS based on complementary structure is proposed in [9]. Meandered metallic pattern is used to design dual-band miniaturized FSS in [10]. A miniaturized dual-band FSS with double square slot element is proposed in [11]. Miniaturized dual-bandstop FSS based on anchor-shaped loop unit-cell structure is proposed in [12]. Miniaturized dual-band FSS based on crooked cross structure is introduced in [13, 14]. Fractal structures [15,16] are also adopted to realize miniaturized dual-band FSSs. Dual-band miniaturized FSS composed of 2-D periodic arrays of subwavelength inductive wire grids and capacitive patches separated by dielectric substrates is introduced in [17]. Nevertheless, most of the FSSs are designed to be band-stop, especially for the convoluted metallic structures, which is unsuitable to design band pass radomes. Also, unit size of the aforementioned FSSs is needed to be decreased.

To solve this problem, a miniaturized dual-band FSS composed of branched tortuous pattern of cross-dipole element backed by wire grid is proposed. By introducing the backing wire grid, the metallic line based FSS can provide two independent pass bands and has smaller unit size compared with other similar structures.

II. FSS STRUCTURE AND ITS EQUIVALENT CIRCUIT MODEL

A. Description of the FSS structure

As shown in Fig. 1 (a), the two FSS layers are separated by a thin dielectric substrate. The first FSS layer is composed of branched tortuous pattern of cross-dipole element and the second one is composed of wire grid. As discussed in [7,8], the miniaturization characteristic can be obtained by increasing the resonant

length of FSS element. Based on this idea, tortuous pattern is adopted to lengthen the resonant length. Meanwhile, branched structure is used to provide two independent resonant paths marked by a red and a blue dash line in Fig. 1 (b), respectively, which will result in two independent frequency bands.
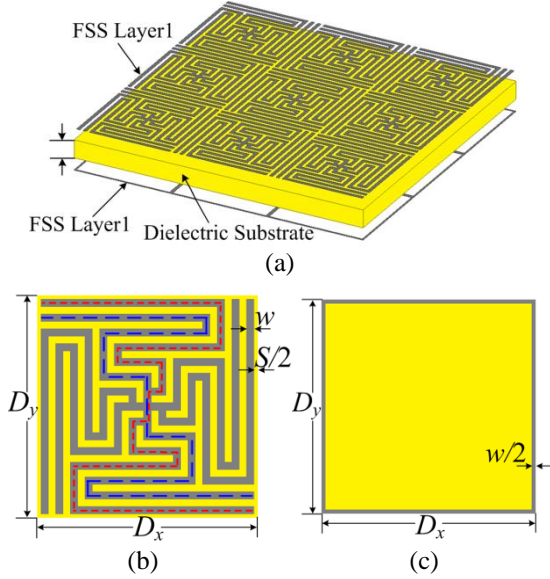
Fig. 1. Structure of the proposed FSS. (a) Perspective view. (b) Top view of unit cell of FSS layer1. (c) Top view of unit cell of FSS layer2.

B. Equivalent circuit model of the proposed FSS

Based on the equivalent circuit theory, the branched tortuous pattern of cross-dipole element can be modelled by the parallel of two series LC resonators and the wire grid can be treated as an inductor L_0. Meanwhile, a short transmission line can be used to depict the thin dielectric substrate. Hence, the proposed FSS can be described by the equivalent circuit model shown in Fig. 2 (a). In our design, thickness of the substrate is relatively small. For simplicity, the dielectric substrate can be modelled as an inductor $L_t = \mu_0\mu_r h$, where μ_r is the relative permeability. Then the equivalent circuit model in Fig. 2 (a) can be simplified into that in Fig. 2 (b).

As indicated in Fig. 2 (b), there will be two stop bands if the two series LC resonators (L_1-C_1 and L_2-C_2) resonate, and the resonant frequencies of passbands can be estimated approximately by the equivalent circuit model. When the first series LC resonator (L_1-C_1) and the inductors (L_0 and L_t) resonate, a pass band will be produced around,

$$f_{p1} \approx 1/2\pi\sqrt{(L_1 + L_0 + L_t)C_1}.$$ (1)

Assuming that the two pass bands are apart, the second pass band will be produced between the two stop bands, whose resonant frequency is around,

$$f_{p2} \approx \frac{1}{2\pi}\sqrt{(C_1 + C_2)/(L_1 + L_2)C_1 C_2}.$$ (2)

Based on the discussion above, it can be found that the proposed FSS can produce two pass bands separated by two transmission zeroes.
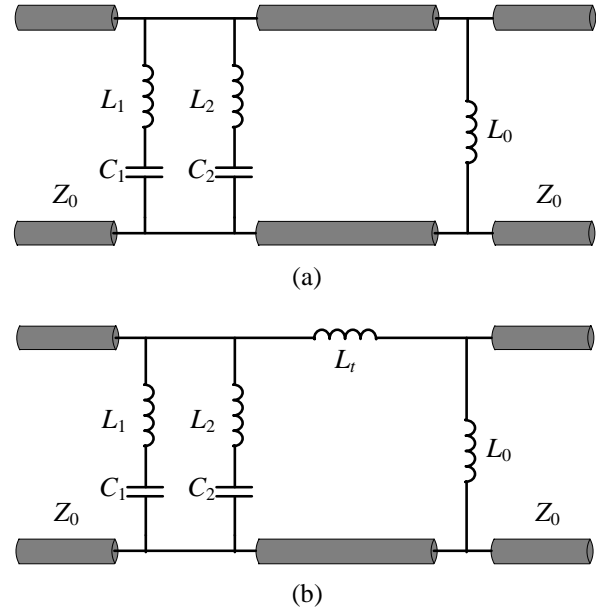
Fig. 2. Equivalent circuit model of the proposed FSS structure. (a) The transmission line model. (b) The lumped-element model.

III. SIMULATION RESULTS

To verify the performance of the proposed FSS, simulations by full-wave solver HFSS and equivalent circuit model have been carried out. As shown in Fig. 1, structure parameters of the proposed FSS are set as follows: dimension of the FSS are $D_x=D_y=6$mm, width of the metallic line is $w=0.2$mm, width of the slot between metallic lines is $s=0.2$mm. The two FSS layers are separated by a F4B-2 substrate. And the dielectric permittivity, tangent loss and thickness of substrate are $\varepsilon_r=2.65$, $tan\delta=0.002$ and $h=0.5$mm, respectively.

First, to explain the forming mechanism of the dual-band characteristic, the two metallic arrays are simulated separately and jointly. The transmission coefficients under normal incidence are shown in Fig. 3. As observed, the proposed FSS structure can provide two stopbands and two passbands. The stopbands operating at 4.54GHz and 6.52GHz are mainly formed by the top metallic array. Due to the existence of the bottom metallic array, the first passband operating at 3.75 GHz is formed. At the same time, the second passband produced by upper FSS is shifted under the influence of wire grid.
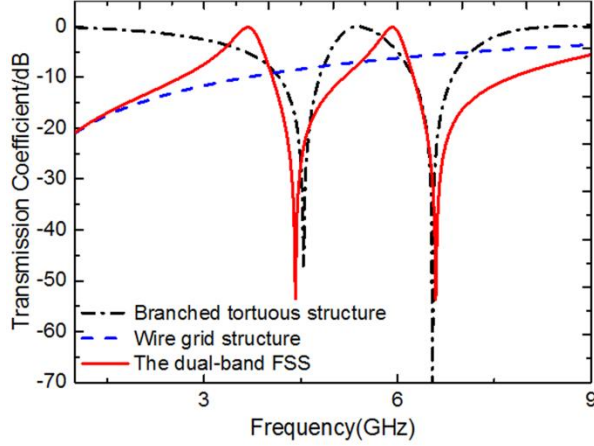
Fig. 3. Transmission coefficients of the constituting metallic arrays and the proposed FSS structure.
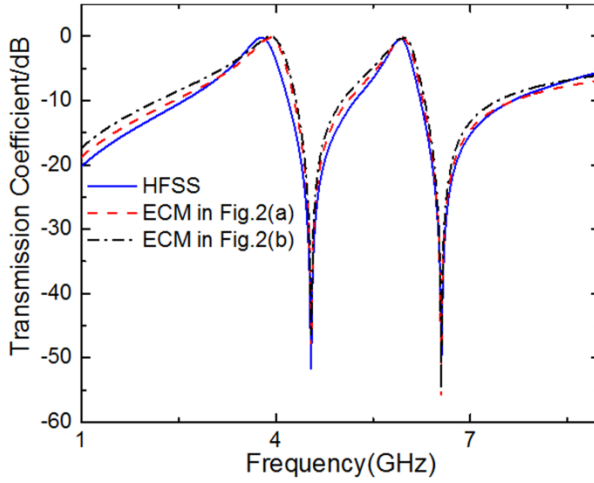
Fig. 4. Transmission coefficient of the proposed FSS at normal incidence.

After that, equivalent circuit method (ECM) is used to obtain the transmission coefficient of the proposed structure. The equivalent circuit parameters of the branched tortuous pattern of cross-dipole element (L_1, C_1, L_2 and C_2) and the wire grid (L_0) are derived from the simulated impendence Z_{FSS} using an iterative procedure proposed in [18]. To reduce the computational burden, two nulls of the impendence Z_{FSS} are used. Corresponding to such two resonances, a well-known relation $L = 1/\omega_{zero}^2 C$ can be obtained. Then, a curve fitting technique based on particle swarm optimization algorithm is applied for extracting parameters. The calculated lumped parameters are L_1=14.6nH, C_1=0.084pF, L_2=11.8nH, C_2=0.051pF, L_0=3.4nH and L_t=0.63nH, respectively.
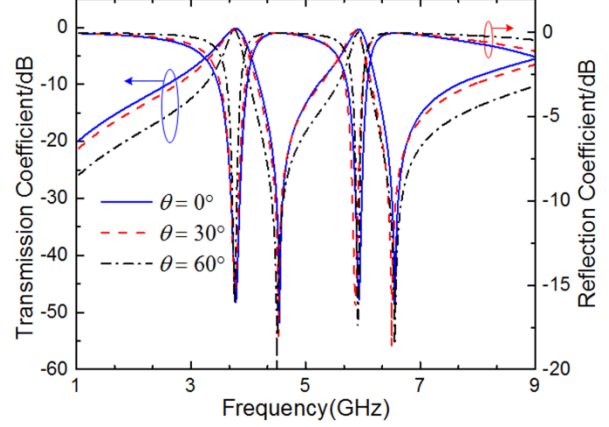
(a)
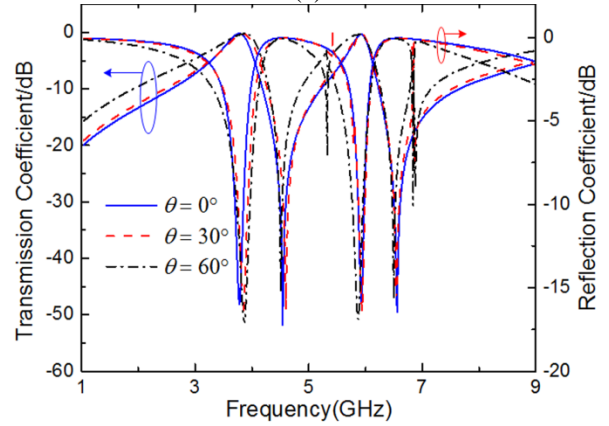
(b)

Fig. 5. Transmission coefficients of the proposed FSS under different incident. (a) TE polarization and (b) TM polarization.

The transmission coefficient under normal incidence can be calculated by equivalent circuit model in Fig. 2 using Eq. (6) in [18]. The calculated transmission coefficient is shown in Fig. 4 together with the simulated one obtained by HFSS. It can be observed that the results obtained by the two methods agree well, which verifies the validity of the equivalent circuit model in Fig. 2. The main discrepancy is the first resonant frequency shift. It is caused by the coupling effect between the two FSS layers, which is not taken into consideration by the equivalent circuit model.

Additionally, the transmission and reflection coefficients of the proposed structure under different incident angles and polarizations are obtained. The results are shown in Fig. 5. Apparently, the proposed structure shows good polarization stability and angular stability. However, as shown in Fig. 5 (b), there are some distortions and spurious resonances for TM polarization of 60° incidence. This is mainly caused by the top

metallic layer. The structure composed of branched tortuous pattern connected in the center will produce the end load capacitance, which is similar with the Jerusalem Cross element. As introduced in [1], because of the existence of end load capacitance, bent mode will be produced for only TM-wave oblique incidence and then a transmission null will be formed. Owing to the branched structure design, there will be two transmission nulls. Noting that the two spurious resonances are away from the passbands, the effect of spurious resonances on frequency filter property can be ignored.
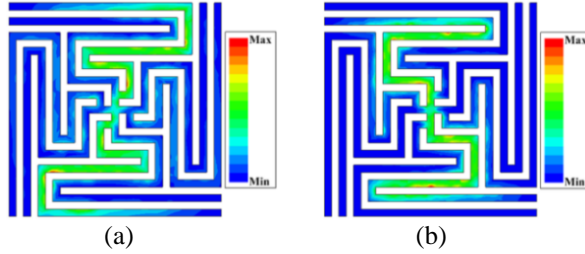
Fig. 6. Surface current distribution diagram. (a) At f=4.54GHz and (b) at f=6.52GHz.

Also, the surface current distribution is given in Fig. 6. It can be observed that the proposed FSS has two stop bands operating at 4.54GHz and 6.52GHz, respectively. Based on the discussion in Section II, the two stop bands are caused by the two resonant paths provided by the branched tortuous structure. For verification, surface current distribution of the branched tortuous structure under normal incidence with TEM wave at 4.54GHz and 6.52GHz are simulated with HFSS and shown in Fig. 6. It can be observed that the branched structure can provide two independent resonant paths as predicted.

There is one point that should be emphasized: the resonant frequencies of the proposed FSS can be adjusted by changing resonant lengths. By increasing the arrangement periodicity, tortuous degree can be improved to fill the FSS unit cell, and then longer resonant lengths are obtained, which will lead to lower resonant frequencies. To further demonstrate this point, several structures with different resonant lengths are simulated under TE polarization. It should be noted that only the resonant lengths and the periodicity of the proposed structure have changed. The transmission coefficients are shown in Fig. 7. The results are tabulated in Table 1, where L_{red} and L_{blue} represent the length of two resonant paths shown in Fig. 1 (b), respectively. And the frequencies f_1 and f_2 represent the positions of the two pass bands. It can be found that the location of pass band will move toward lower frequency as the resonant lengths increase.

To further verify the performance of the proposed FSS, comparisons between previous works have been carried out. It can be observed from Table 2, unit size of

the proposed FSS is smaller compared with other similar structures, which demonstrates that the proposed FSS is a better miniaturized design. Also, based on Eq. (1.5) in [1], the lowest onset frequency of grating lobe of 60° incidence is 26.8GHz, which is far from the resonant frequency.
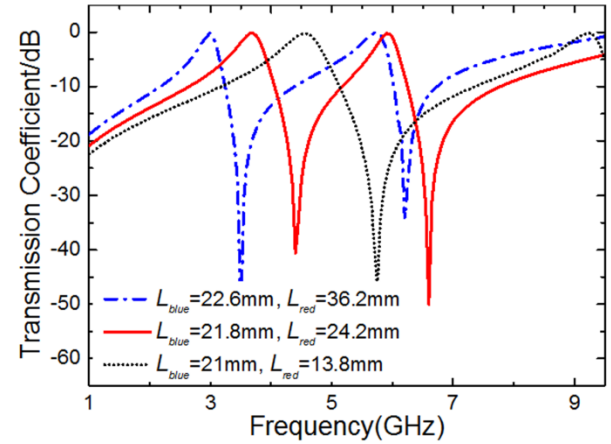
Fig. 7. Transmission coefficient of proposed structure with different resonate lengths.

Table 1: Length of two resonant paths and resonant frequencies of two pass bands

L_{blue} (mm)	L_{red} (mm)	$D_x=D_y$ (mm)	f_1 (GHz)	f_2 (GHz)
21	13.8	2.6	4.55	9.24
21.8	24.2	3	3.75	5.88
22.6	36.2	3.4	2.99	5.68

Table 2: Comparisons with other dual-band FSSs

ε_r	FSS Structure	FSS Unit Size
2.65	FSS structure in [11]	0.1407λ×0.1407λ
	FSS structure proposed	0.075λ×0.075λ
4.4	FSS structure in [13]	0.0826λ×0.0826λ
	FSS structure in [13]	0.088λ×0.088λ
	FSS structure in [13]	0.094λ×0.094λ
	FSS structure proposed	0.0616λ×0.0616λ

IV. EXPERIMENTAL VERIFICATION

An FSS prototype has been fabricated and measured (see Fig. 8) for further verification. The prototype is consisting of 60×60 elements and the oversize is 362mm×362mm. The FSS prototype is measured with a free-space method in an anechoic chamber. The free-space measurement system is mainly composed of a transmitting antenna and a receiving antenna, which are connected to a vector network analyzer (Agilent E8363B). And the transmitting antenna and the receiving antenna are placed on each side of the prototype with a

distance of 2m and 0.8m, respectively.

(a)   (b)
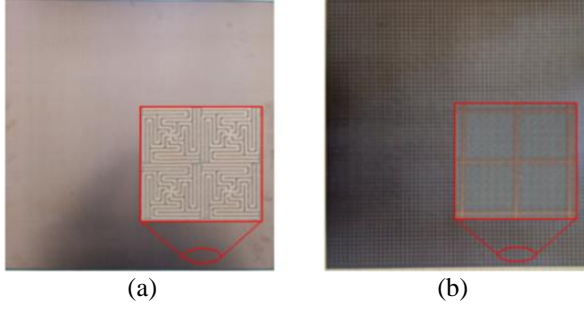
Fig. 8. Photograph of the FSS prototype. (a) FSS layer1 and (b) FSS layer 2.

(a)

(b)
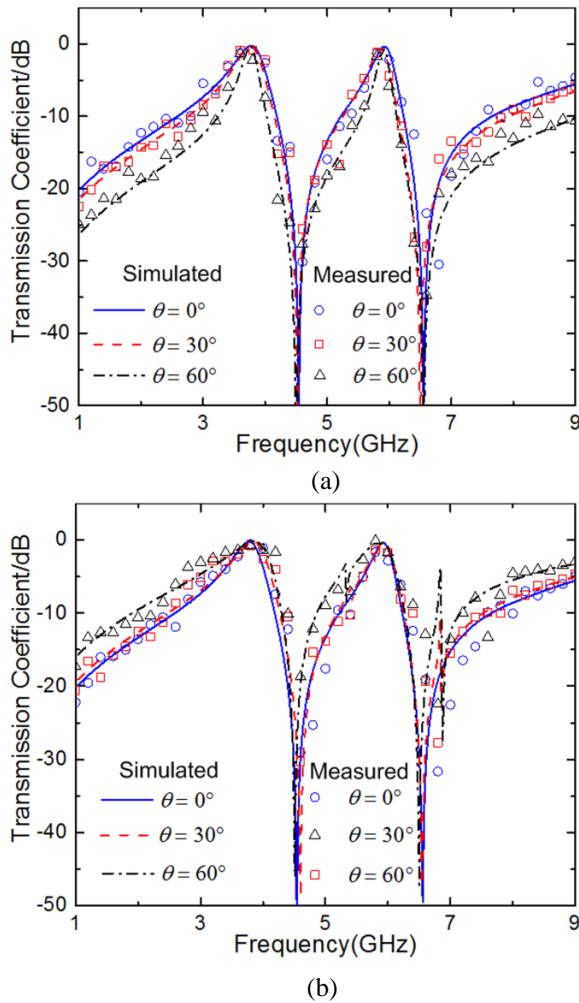
Fig. 9. Comparisons between the simulated and the measured transmission coefficients. (a) TE polarization and (b) TM polarization.

Comparisons between the measured and simulated transmission coefficients are shown in Fig. 9. Good agreements between the two methods can be observed,

which demonstrates the validation of the proposed FSS structure design. And the reason causing spurious resonances has been explained above.

The passbands for simulation, ECM, and measurement under TE polarization are tabulated in Table 3. As observed, the results obtained by three methods are highly consistent. For ECM, the resonant frequency deviation respect to HFSS is slightly larger, which is 3.47% and 1.02%, respectively. This is because the coupling between upper and lower metallic layers of proposed structure is ignored. For measurement, the resonant frequency deviation is only 0.27% and 0.51%.

Table 3: The passbands obtained by three methods

Resonant Frequency	HFSS	ECM	Measurement
f_1 (GHz)	3.75	3.88	3.76
f_2 (GHz)	5.88	5.94	5.91

V. CONCLUSION

In this paper, a miniaturized dual-band band pass FSS is designed using a branched tortuous structure. The proposed FSS is analyzed, fabricated and measured. Both simulated and measured results show that the proposed FSS has smaller unit size compared with other similar structures and its unit size is only $0.075\lambda \times 0.075\lambda$. Also, it has a better angular stability at oblique incidence and the resonant frequency deviation for the two pass bands keeps below 2% of 60° incidence under different polarizations. The proposed FSS can be applied for FSS radomes.

ACKNOWLEDGMENT

REFERENCES

[1] B. A. Munk, *Frequency Selective Surface: Theory and Design*. John Wiley & Sons, 2005.

[2] R. Mittra, C. H. Chan, and T. Cwik, "Techniques for analyzing frequency selective surfaces-A review," *Proceedings of the IEEE*, vol. 76, no. 12, pp. 1593-1615, 1988.

[3] F. Costa and A. Monorchio, "A frequency selective radome with wideband absorbing properties," *IEEE Transactions on Antennas Propagation*, vol. 60, no. 6, pp. 2740-2747, 2012.

[4] H. Chen, X. Hou, and L. Deng, "Design of frequency selective surfaces radome for a planar slotted waveguide antenna," *IEEE Antennas and Wireless Propagation Letters*, vol. 8, pp. 1231-1233, 2009.

[5] M. Yan, J. Wang, H. Ma, *et al.*, "A tri-band, highly selective, bandpass FSS using cascaded multilayer loop arrays," *IEEE Transactions on Antennas Propagation*, vol. 64, no. 5, pp. 2046-2749, 2016.

[6] K. Sarabandi and N. Behdad, "A frequency selective surface with miniaturized elements," *IEEE Transactions on Antennas Propagation*, vol. 55, no. 5, pp. 1239-1245, 2007.

[7] N. Liu, X. J. Sheng, and J. J. Fan, "A compact miniaturized frequency selective surface with stable resonant frequency," *Progress In Electromagnetics Research Letters*, vol. 62, pp. 17-22, 2016.

[8] N. Liu, X. J. Sheng, J. J. Fan, and D. M. Guo, "A miniaturized FSS based on tortuous structure design," *IEICE Electronics Express*, vol. 14, no. 2, pp. 20161129, 2017.

[9] X. D. Hu, X. L. Zhou, L. S. Wu, *et al.*, "A miniaturized dual-band frequency selective surface (FSS) with closed loop and its complementary pattern," *IEEE Antennas and Wireless Propagation Letters*, vol. 8, pp. 1374-1377, 2009.

[10] F. C. Huang, C. N. Chiu, T. L. Wu, *et al.*, "Very closely located dual-band frequency selective surfaces via identical resonant elements," *IEEE Antennas and Wireless Propagation Letters*, vol. 14, pp. 414-417, 2015.

[11] Y. Yang, X. H. Wang, and H. Zhou, "Dual-band frequency selective surface with miniaturized element in low frequencies," *Progress In Electromagnetics Research Letters*, vol. 33, pp. 167-175, 2012.

[12] M. Yan, S. Qu, J. Wang, *et al.*, "A miniaturized dual-band FSS with stable resonance frequencies of 2.4 GHz/5 GHz for WLAN applications," *IEEE Antennas and Wireless Propagation Letters*, vol. 13, pp. 895-898, 2014.

[13] C. N. Chiu and W. Y. Wang, "A dual-frequency miniaturized–element FSS with closely located resonances," *IEEE Antennas and Wireless Propagation Letters*, vol. 12, pp. 163-165, 2013.

[14] R. Sivasamy and M. Kanagasabai, "A novel dual-band angular independent FSS with closely spaced frequency response," *IEEE Microwave and Wireless Components Letters*, vol. 25, no. 5, pp. 298-300, 2015.

[15] T. Zhong, H. Zhang, R. Wu, *et al.*, "A single-layer dual-band miniaturized frequency selective surface with compact structure," *IEEE Asia-Pacific International Symposium on Electromagnetic Compatibility*, pp. 122-124, 2016.

[16] Y. Y. Lv and W. L. Chen, "Dual-polarized multiband frequency selective surface with miniaturized Hilbert element," *Microwave and Optical Technology Letters*, vol. 55, no. 6, pp. 1221-1223, 2013.

[17] M. Gao, S. M. A. M. H. Abadi, and N. Behdad, "A dual-band inductively coupled miniaturized-element frequency selective surface with higher order bandpass response," *IEEE Transactions on Antennas Propagation*, vol. 64, no. 8, pp. 3729-3734, 2016.

[18] F. Costa, A. Monorchio, and G. Manara, "Efficient analysis of frequency-selective surfaces by a simple equivalent-circuit model," *IEEE Transactions on Antennas Propagation*, vol. 54, no. 4, pp. 35-48, 2012.

Ning Liu received his B.S. degree in Electronic and Information Engineering from Dalian University of Technology, Dalian, China, in 2013. He is currently working towards the Ph.D. degree in Mechanical Engineering, Dalian University of Technology. His research interests include Metamaterials, Frequency selective surface design and analysis, Antenna radome, and computational electromagnetics.

Xianjun Sheng was born in Liaoning, China, in 1969. She received her M.S. and Ph.D. degrees from Dalian University of Technology, Dalian, China, in 1997 and in 2003, respectively. She works currently as a Professor in Department of Electrical Engineering, Dalian University of Technology. Her research interests include Antenna radome, Computational electromagnetics and Control theory.

Xiang Gao received his B.S. degree in Electrical Engineering, Dalian Jiaotong University China, in 2017. He is currently working towards the M.S. degree in Electrical Engineering in Dalian University of Technology. His research interest is Frequency selective surface design and analysis.

Chunbo Zhang received his M.S. degree in Electrical Engineering from Shengyang University of Technology, China, in 2004. He received his Ph.D. degree from Dalian University of Technology, Dalian, China, in 2008. He is currently working as Senior Engineer in Research Institute of Aerospace Special Materials and Processing Technology, China. His research interests include antenna radome, design and analysis of metamaterials.

Dongming Guo received his Ph.D. degree in Mechanical Engineering from Dalian University of

Technology, Dalian, China, in 1992. He is currently working as a Professor in Department of Mechanical Engineering in Dalian University of Technology. His research interests include Antenna radome, Metamaterials, special machining and precision machining technology and digital design and manufacturing.